# Directly Rolling Nanosheets into Nanotubes

**Renzhi Ma,* Yoshio Bando, and Takayoshi Sasaki**

*Advanced Materials Laboratory, National Institute for Materials Science, Namiki 1-1, Tsukuba, Ibaraki 305-0044, Japan*

*Received: October 23, 2003; In Final Form: January 5, 2004*

We report a process directly transforming 2D nanosheets into 1D nanotubes. Using unilamellar nanosheets as starting materials, we succeeded in obtaining titanium oxide, manganese oxide, and niobate nanotubes (15−60 nm in diameter). The transformation was achieved in a simple procedure of an ion intercalation/deintercalation procedure at ambient temperature. The intercalation of Na ions leads to stacking up of the colloidal nanosheets. The gradual deintercalation/extraction of Na ions in water changes the inter-sheet bonding character. The peeled off nanosheets naturally roll up into nanotubes. It is most likely to be a universal process and has outstanding potential in customized syntheses of nanotubes from a wide range of lamellar solids.

## Introduction

Nanoscale structures have attracted immense interest in recent years.[1−4] Thanks to the steadily increasing synthetic capabilities, a so-called "nano-toolbox" filled with a variety of nanocrystallites including nanoparticles/quantum dots (zero-dimension, 0D), nanotubes/nanorods/nanobelts (one-dimension, 1D), and nanosheets (two-dimension, 2D), have been explored.[1−6] Especially, 1D nanotubes are subjects of particular interest owing to their unique atomic structures and great potential in electronic, optical, mechanical, and bioscience applications. Diverse synthetic routes have been directed to 1D nanotube growth. Most of the synthesized nanotubes, represented by carbon, boron nitride, oxides, and metal dichalcogenides, commonly possess layered/lamellar structures.[3,4] The formation of a hollow tube, consisting of concentric cylinders or scrolls of molecular sheets, may be modeled as the rolling and folding up of a sheet onto itself, i.e., a 2D-to-1D structure transformation. It is thus a long belief that all the lamellar solids could form tubular structures only if proper conditions are offered.

A variety of lamellar solids have been successfully exfoliated/delaminated into single-layer nanosheets through soft chemical procedures.[5−11] Mallouk and co-workers observed spontaneous nanotube formation in the exfoliated nanosheets of some particular hexaniobates and Ruddlesden−Popper phases of layered perovskites.[12,13] The driving force appears to be relief of built-in strain due to noncentrosymmetry architecture in individual sheets or the change of intrinsic bonding character between neighboring layers. Some authors have also investigated the formation of $WS_2$ and $VO_x$ nanotubes in hydrothermal procedures assisted by organic templates.[14,15] They obtained nanotubes together with some sheetlike crystallites with lateral curling or bending, implying a possible "rolling mechanism" from the sheets to nanotubes. Inspired by these intriguing discoveries, is it possible to develop a generalized and controlled procedure to intentionally roll 2D nanosheets into 1D nanotubes directly, similar to the way of rolling up a thin film?[16] If such a formation scenario can be really realized, it will be a significant breakthrough for nanotube synthetic methods taking in account the wide availability of a big family of exfoliated 2D nanosheets.

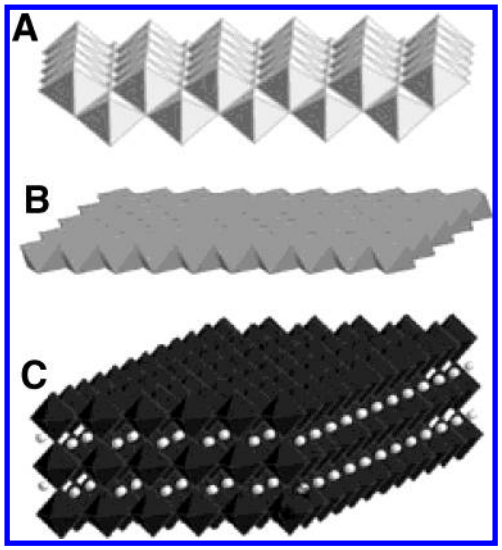


**Figure 1.** The architectures of 2D nanosheets of (A) $Ti_{0.91}O_2$, (B) $MnO_2$, and (C) $Ca_2Nb_3O_{10}$.

Here we report a probable generalized method rolling 2D nanosheets into 1D nanotubes. Three kinds of colloidal nanosheets, $Ti_{0.91}O_2$,[6] $MnO_2$,[9] and $Ca_2Nb_3O_{10}$[11] were used as the starting materials. Titanium oxide and niobate are useful in photochemical and photocatalytic applications owing to their semiconducting nature. Layered manganese oxide with a feasible redox capability holds promise for a range of applications including energy storage and new solar cells. In our method, a simple two-step procedure was explored based on ion intercalation/deintercalation at ambient temperature. The intercalation of Na ions leads to the stacking of the unilamellar nanosheets. The gradual deintercalation/extraction of Na ions from the restacked nanosheets in water induces driving force for nanotube formation.

* Author to whom correspondence should be addressed. Fax: 81-29-851-6280. E-mail: MA.Renzhi@nims.go.jp.

10.1021/jp037200s CCC: $27.50 
Published on Web 01/24/2004

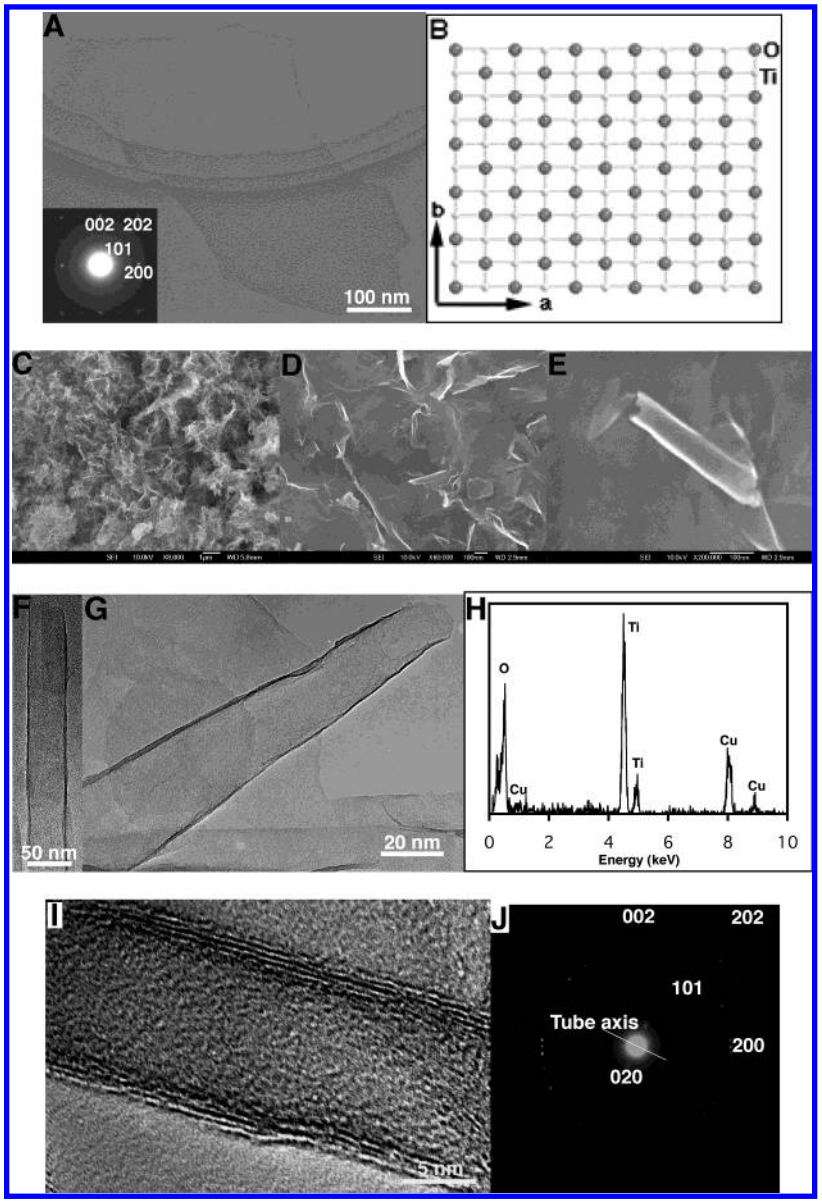


**Figure 2.** The formation of titanium oxide nanotubes. (A) Starting 2D nanosheet (inset) ED pattern. (B) Atomic model of the nanosheet along [010] projection. (C) flocculated nanosheets using NaOH solution. (D,E) Nanosheets after 36 h water washing, note the formation of needle-shaped crystallities. (F,G) TEM images of typical straight and conical nanotubes. (H) EDS measurement identifying there is no residual $Na^+$. (I) HRTEM image showing the ~8 Å interlayer distance in the tube walls. (J) ED pattern of the nanotube. The tube axis is depicted as shown.

## Experimental Section

**Materials.** All the nanosheets were prepared in a well-established soft chemical procedure involving proton exchange, and subsequent $TBA^+OH^-$ intercalation.[6−11] Starting lamellar solids of lepidocrocite-type cesium titanate $Cs_{0.7}Ti_{1.825}\square_{0.175}O_4$ ($\square$ represents a vacancy),[17] birnessite-type potassium manganese oxide $K_{0.45}MnO_2$,[18] and perovskite-type niobate $KCa_2Nb_3O_{10}$ (known as Dion-Jacobson phase)[19,20] were synthesized via conventional solid-state calcination. Subsequent acid leaching converted them into protonated forms of $H_{0.7}Ti_{1.825}\square_{0.175}O_4 \cdot H_2O$, $H_{0.13}MnO_2 \cdot 0.7H_2O$, and $HCa_2Nb_3O_{10} \cdot 1.5H_2O$, respectively. The resulting protonic product (0.4 g) was shaken vigorously in 100 $cm^3$ of an aqueous tetrabutylammonium hydroxide ($TBA^+OH^-$) solution at ambient temperature for ~2 weeks. The obtained stable colloidal suspensions consist of exfoliated single-layer nanosheets of hydrated $Ti_{0.91}O_2$, $MnO_2$, and $Ca_2Nb_3O_{10}$ with molecular thickness of approximately 0.75, 0.60, and 1.44 nm, respectively.[6,9,11] The architectures of these single nanosheets are illustrated in Figure 1. $MO_6$ (M = Ti, Mn, Nb) octahedra are combined via edge or corner sharing to produce 2D arrays. The lateral dimensions of these nanosheets generally range 0.1−1 $\mu$m.

**Transformation.** The colloidal nanosheets underwent flocculation/restacking by changing ionic strength. Typically, 30 $cm^3$ of colloidal suspension was poured into 30 $cm^3$ of NaOH aqueous solution (1 mol $dm^{-3}$). Wool-like precipitate was yielded and the mixture was maintained overnight under stirring. After filtration, the resulting material was rinsed with copious distilled water, and then shaken in 100 $cm^3$ distilled water. The distilled water was changed to a fresh one after every 12 h. A well-dispersed suspension was achieved generally after more than 36 h shaking. The final product was collected from centrifugation, and then air-dried at room temperature.

**Characterization.** The products were characterized by a number of different methodologies, including X-ray diffraction (XRD, Cu K$\alpha$), scanning electron microscopy (SEM), trans-

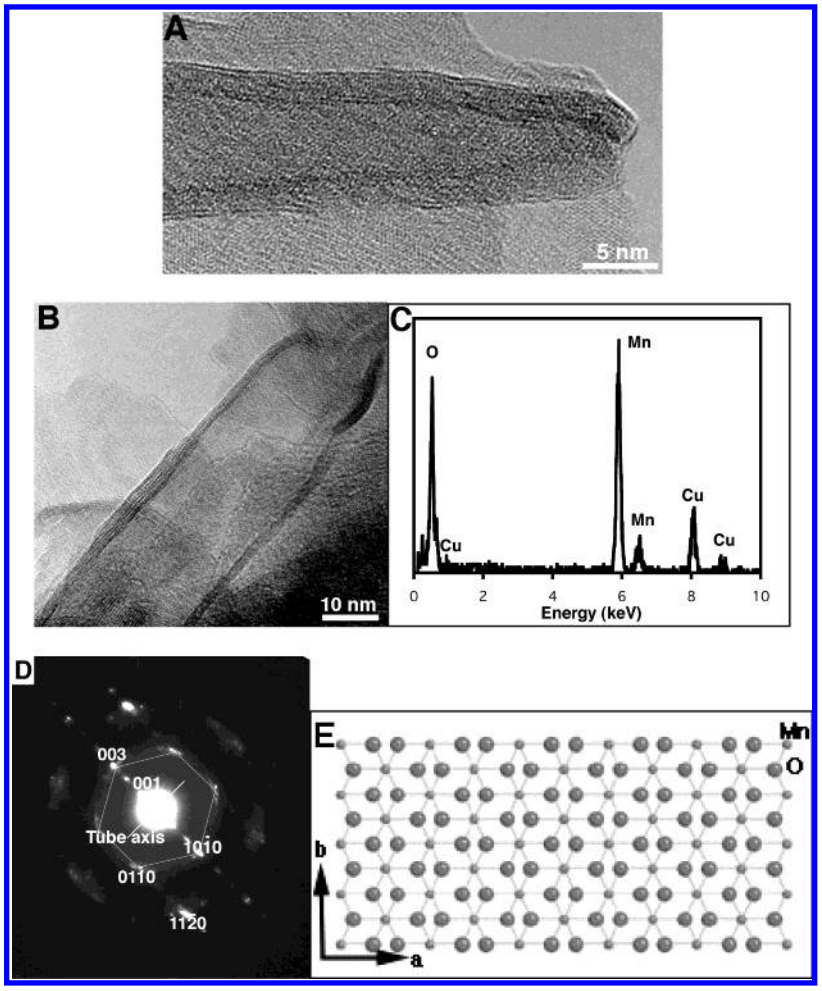


**Figure 3.** The formation of manganese oxide nanotubes. (A,B) TEM images of typical straight and conical nanotubes. (C) EDS measurements identifying the absence of residual $Na^+$. (D) Typical ED pattern of the $MnO_2$ nanotube showing the {000l} basal nodes and hexagonal arrangement of {10$\bar{1}$0} spots. The tube axis is generally along [1$\bar{2}$10]. (E) Atomic model of the $MnO_2$ sheet along [0001] projection.

mission electron microscopy (TEM) combined with energy-dispersive spectroscopy (EDS), and electron energy loss spectroscopy (EELS).

## Results and Discussion

Figure 2A depicts the typical TEM image of the starting $Ti_{0.91}O_2$ nanosheets. The nanosheet exhibits a uniform and faint contrast, reflecting unilamellar thickness. The ED pattern from a single sheet (inset) indicates the face-centered rectangular unit cell of the single-crystal sheet ($a = 3.783$ Å, $c = 2.978$ Å).[6,21] Figure 2B illustrates the atomic model of the nanosheet along [010] projection.

The flocculation of the colloidal nanosheets in NaOH solution led to a porous aggregate (Figure 2C). The XRD patterns of the flocculated products were basically comprised of {0*k*0} basal series and {*h*0*l*} reflections, indicating the absence of a three-dimension order. This suggests that the flocculation results in turbostratic restacking of the single-layer nanosheets that accommodate Na ions and water molecules between the neighboring sheets.[11] On the basis of the microscopic characterization, turbostratic stacks of 5−20 nanosheets appear dominant in the flocculated product. The morphology of the product after filtering and shaking in water is shown in Figure 2D,E. The restacked nanosheets were partially delaminated again and well dispersed. Most of the dispersed nanosheets exhibit lateral curling. Some needle-shaped objects are also observed. TEM observations demonstrate clearly that the needle-shaped crystallites are nanotubes with apparent hollow core. The nanotubes could be very straight (Figure 2F) or conical (Figure 2G). The diameter of a selected tube was monitored when it was tilted along the tube axis. The diameter was found to remain constant for different tilting angles (∼30°) about its axis, identifying the true tubular nature and not wrinkles of the sheets. EDS and EELS measurements conclude that there is no residual $Na^+$ (detection limit 2%) in these nanotubes. Figure 2H gives the typical EDS measurement, demonstrating the existence of only Ti and O (Ti/O ∼ 1:2; the Cu peaks are derived from the copper grid). Taking into account the possible $H^+$, the nanotubes are likely to be protonic titanium oxide.

HRTEM images indicate that the tube walls are usually very thin, only 3∼6 layers. The interlayer distance in the nanotubes is ∼8.0 Å (Figure 2I), smaller than the (002) inter-planar spacing (9.4 Å, $b = 18.735$ Å) in starting protonated titanate.[6] This might be due to shrinkage of interlayer distance as a direct consequence of the loss of hydrated water in high vacuum during microscopic observations. Figure 2J is the electron diffraction (ED) pattern corresponding to the nanotube in Figure 2I. Some weak reflection rings in the pattern are ascribed to the underlying sheets beneath the tube. The primary diffraction spots with relatively strong intensities are indexed to be two (020) nodes at the edge of the zero spot and streaked {*h*0*l*} reflections, a typical diffraction pattern of tubular structures.[22] The tube axis is perpendicular to the row of (020) reflections, as depicted in Figure 2J, and the electron beam is incident at the central region

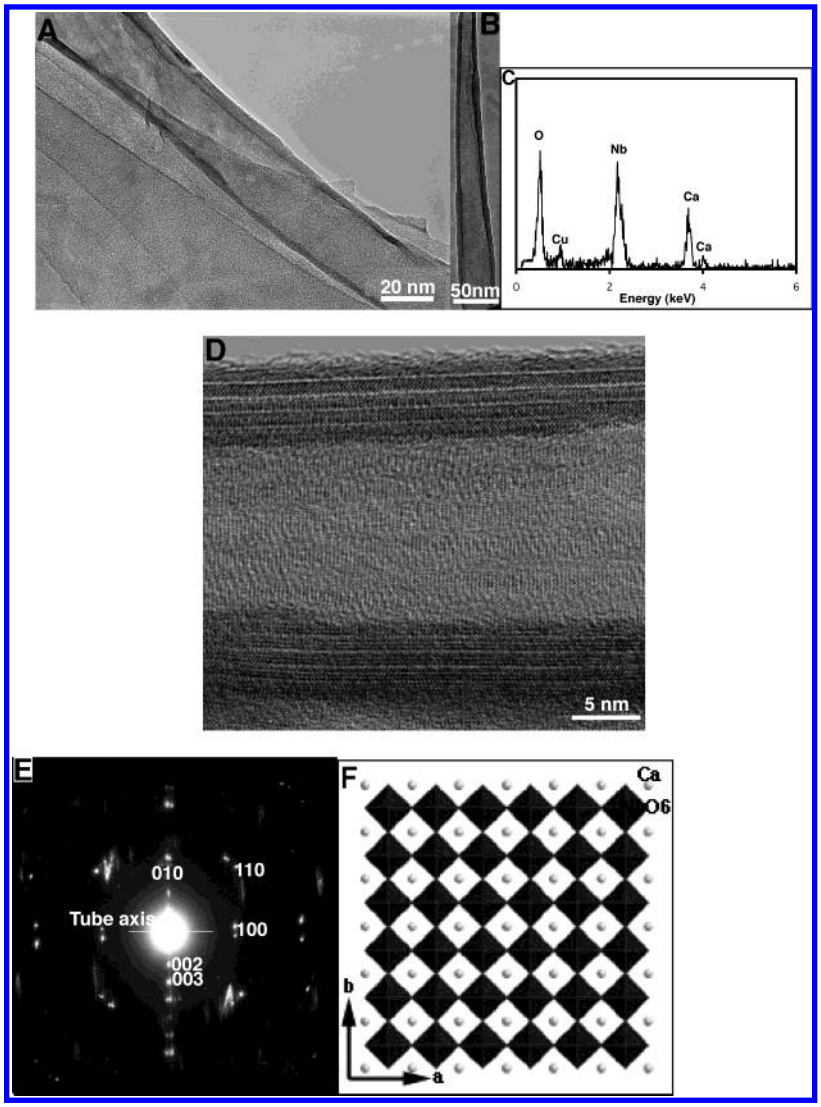


**Figure 4.** The formation of niobate nanotubes. (A,B) TEM images of typical straight and conical nanotubes. (C) Typical EDS measurement. (D) HRTEM image of a nanotube, the wall layers are separated by a 14.4 Å repeated distance. (E) ED pattern demonstrating that the nanotube may be constructed by wrapping a sheet of $Ca_2Nb_3O_{10}$ along [001] with the tube axis parallel to [100]. (F) Atomic model of $Ca_2Nb_3O_{10}$ projected along [001].

of the tube (the top and bottom sheets tangent to the tube and normal to the incident beam) along [010]. It thus can be deduced that this scroll-type tube may be constructed by wrapping up a 2D sheet along [010] with the depicted tube axis.

Figure 3 shows the nanotubes obtained from $MnO_2$ nanosheets. There are also two types of nanotubes, straight and conical ones, were attained (Figure 3A,B). The elemental composition by EDS and EELS confirmed the absence of $Na^+$ in the nanotubes (see a typical EDS in Figure 3C). The ED pattern in Figure 3D recorded on an individual nanotube also clearly exhibits reflection characteristic of a tubular structure. The interlayer distance in the tube walls is 7.3 Å, consistent with (0001) interplanar spacing in layered protonic manganese oxide. The $MnO_2$ nanosheet can be regarded as a 2D array with a hexagonal unit cell ($a \approx 2.90$Å).[9,18] The atomic model of the nanosheets projected along [0001] is shown in Figure 3E. The arrangement of the in-plane $\{10\bar{1}0\}$ spots in Figure 3D also evidences the hexagonal feature (There is an overlap between (0003) and $(10\bar{1}0)$ spots due to the close $d$ values: $d(0003) = 2.43$ Å, $d(10\bar{1}0) = 2.51$ Å). It is a common feature that the nodes degenerate into streaks, indicative of the tubular morphology and possible helicity.[22] The incident electron beam is on the central region of the nanotube along [0001] and the tube axis is perpendicular to the row of (000l) reflections. In this ED pattern, the tube axis appears also generally perpendicular to $[10\bar{1}0]$. We therefore can suggest that the tube axis might be parallel to $[1\bar{2}10]$. A model $MnO_2$ nanotube may be formed via rolling up the sheet along [0001] normal in a tube axis parallel to $[1\bar{2}10]$.

Figure 4 shows the TEM characterization of $Ca_2Nb_3O_{10}$ nanotubes. Again, both straight and conical nanotubes were observed (Figure 4A,B). There is also no detectable residual $Na^+$ (Figure 4C). The HRTEM image of a typical nanotube in Figure 4D shows the well-resolved layer arrangement in the tube walls. The interlayer distance is approximately 14.4 Å, corresponds to the $d(001)$ of protonic niobium oxide.[23] The $Ca_2Nb_3O_{10}$ nanosheets are comprised of a square unit cell ($a = b = 3.854$ Å). On the basis of the ED pattern taken from an individual nanotube (Figure 4E), it can be concluded that the tube is rolled up from the 2D nanosheet (See atomic model in Figure 4F) along [001] normal while the tube axis is parallel to one of the unit cell axis (e.g., [100]). The diffraction spots are also slightly elongated in the direction perpendicular to the tube axis.

All the three types of nanotubes have an outer diameter of 15∼60 nm and a wall thickness of 3∼6 layers. The dimensions

correspond to a scroll from a single 2D sheet with 140∼1130 nm in lateral size, which is consistent with the starting nanosheets (0.1−1 $\mu$m). This indicates that there is no fracture or breakage of the starting nanosheets during the rolling up. As a comparison, it is noteworthy that there are some previous reports on the syntheses of titanium oxide or trititanate ($H_2Ti_3O_7$) nanotubes in hydrothermal or sonochemical treatments (110−150 °C) of $TiO_2$ nanoparticles in concentrated (10 mol $dm^{-3}$) NaOH solution (We recently discovered that the hydrothermal nanotubes might be also of lepidocrocite nature).[24−27] The diameters of those nanotubes are usually 5−10 nm, significantly different from the dimensions in the present study.

The formation of the 1D nanotubes from 2D nanosheets may be explained as follows. The starting unilamellar nanosheets were stabilized in a suspension with $TBA^+OH^-$. During the flocculation using NaOH solution, $Na^+$ substituted for $TBA^+$. The colloidal 2D nanosheets became unstable and got restacked incorporating Na ions. The Na ions were intercalated into the inter-sheet gallery and played a role in pinning the adjacent sheets. This resulted in a porous aggregate of fine crystallites of 5−20 turbostratic layered nanosheets. When shaking in water, the inter-sheet Na ions were gradually deintercalated/extracted. This deintercalation process was realized through the exchange with protons and water molecules ($H_3O^+$), causing the variance in bonding character between adjacent sheets. During shaking, the inter-sheet spacing might also be expanded due to the increase in water contents. The electrostatic interaction between neighboring sheets were thus significantly reduced. As a result, the turbostratic restacked nanosheets became very loosely bonded and were granted a tendency to delaminate into individual nanosheets again. In pure water, the individual nanosheet tends to flocculate within itself as the solution conditions are not perfectly suitable to attain well-dispersed colloids. When the nanosheet flocculates within itself, it needs to be folded. If some particular optimum geometrical requirement is fulfilled, nanotube formation takes place. In other major cases, the nanosheets formed just irregular shaped objects. It is also reasonable to suggest that the deintercalation of Na ions occurred initially from the edge sites in the turbostratic layered nanosheets. The reduction of electrostatic interaction therefore happened first to the lateral edges of the nanosheets. Due to the reduced interaction with underlying layered sheets, the lateral edges of the topmost sheet might gradually curl up, similar to a thin film free from the underlying substrate.[16] With the proceeding of the edge curling-up process, the topmost sheet will be totally peeled off and rolled into multilayer nanotubes. On the basis of microscopy statistics, approximately 20% titanium oxide and manganese oxide nanosheets were transformed into nanotubes. As niobate nanosheets had a larger thickness (1.44 nm) compared with titanium oxide (0.75 nm) and manganese oxide (0.6 nm), they were transformed into nanotubes in a lower yield (∼10%). Further work is underway to optimize the process and increase nanotube purity.

In summary, we succeed in directly rolling 2D nanosheets into 1D nanotubes. The transformation relies on a simple ion intercalation/deintercalation principle at ambient temperature. The success was not only achieved in titanium oxide nanotubes, but also in nanotubes of manganese oxides and niobate for the first time. It directly verifies the assumption of rolling up a molecular sheet into a cylindrical or conical nanotube. It is also likely a universal process to yield 1D nanotubes from 2D nanosheets and applicable to any other lamellar solids only if the exfoliated nanosheets are available.

**Acknowledgment.** R.M. acknowledges Drs. H. Tanaka, L. Wang, and Y. Ebina for providing the colloidal nanosheets of titanium oxide, manganese oxide, and niobate, respectively. This work has been partly supported by CREST of JST (Japan Science and Technology Agency).

## References and Notes

(1) Nalwa, H S. *Handbook of Nanostrucutred Materials and Nanotechnology*; Academic Press: New York, 2000.
(2) Xia, Y.; Yang, P.; Sun, Y.; Wu, Y.; Mayers, B.; Gates, B.; Yin, Y.; Kim, F.; Yan, H. *Adv. Mater.* **2003**, *15*, 353−389.
(3) Patzke, G. R.; Krumeich, F.; Nesper, R. *Angew. Chem., Int. Ed.* **2002**, *41*, 2446−2461.
(4) Rao, C. N. R.; Nath, M. *Dalton Trans*. **2003**, 1−24.
(5) Jacobson, A. J. *Mater. Sci. Forum* **1994**, *152*, 1−12.
(6) Sasaki, T.; Watanabe, M.; Hashizume, H.; Yamada, H.; Nakazawa, H. *J. Am. Chem. Soc.* **1996**, *118*, 8329−8335.
(7) Fang, M.; Kim, C. H.; Saupe, G. B.; Kim, H.; Waraksa, C. C.; Miwa, T.; Fujishima, A.; Mallouk, T. *Chem. Mater.* **1999**, *11*, 1526−1532.
(8) Liu, Z.; Yang, X.; Makita, Y.; Ooi, K. *Chem. Mater.* **2002**, *14*, 4800−4806.
(9) Omomo, Y.; Sasaki, T.; Wang, L.; Watanabe, M. *J. Am. Chem. Soc.* **2003**, *125*, 3568−3575.
(10) Treacy, M. M. J.; Rice, S. B.; Jacobson, A. J.; Lewandowski, J. T. *Chem. Mater.* **1990**, *2*, 279−286.
(11) Ebina, Y.; Sasaki, T.; Harada, M.; Watanabe, M. *Chem. Mater.* **2002**, *14*, 4390−4395.
(12) Saupe, G. B.; Waraksa, C. C.; Kim, H.; Han, Y. J.; Kaschak, D. M.; Skinner, D. M.; Mallouk, T. E. *Chem. Mater.* **2000**, *12*, 1556−1562.
(13) Schaak, R. E.; Mallouk, T. E. *Chem. Mater.* **2000**, *12*, 3427−3434.
(14) Li, Y. D.; Li, X. L.; He, R. R.; Zhu, J.; Deng, Z. X. *J. Am. Chem. Soc.* **2002**, *124*, 1411−1416.
(15) Chen, X.; Sun. X.; Li, Y. *Inorg. Chem.* **2002**, *41*, 4524−4530.
(16) Schmidt, O. G.; Eberl, K. *Nature* **2001**, *410*, 168.
(17) Grey, I. E.; Madsen, I. C.; Watts, J. A. *J. Solid State Chem.* **1987**, *66*, 7−19.
(18) Post, J. E.; Veblen, D. R. *Am. Mineral.* **1990**, *75*, 477−489.
(19) Dion, M.; Ganne, M.; Tournoux, M. *Mater. Res. Bull.* **1981**, *16*, 1429−1435.
(20) Jacobson, A. J.; Johnson, J. W.; Lewandowski, J. T. *Inorg. Chem.* **1985**, *24*, 3727−3729.
(21) Sasaki, T.; Ebina, Y.; Kitami, Y.; Watanabe, M. *J. Phys. Chem. B* **2001**, *105*, 6116−6121.
(22) Zhang, X. B.; Zhang, X. F.; Amelinckx, S.; Tendeloo, G. Van.; Landuyt, J. Van. *Ultramicroscopy* **1994**, *54*, 237−249.
(23) Jacobson, A. J.; Lewandowski, J T.; Johnson, J. W. *J. Less-Common Metals* **1986**, *116*, 137−146.
(24) Kasuga, T.; Hiramatsu, M.; Hoson, A.; Sekino, T.; Niihara, K. *Adv. Mater.* **1999**, *11*, 1307−1311.
(25) Zhu, Y. C.; Li, H. L.; Koltypin, Y. R.; Hacohen, Y. R.; Gedanken, A. *Chem. Commun.* **2001**, 2616−2617.
(26) Chen, Q.; Du, G. H.; Zhang, S.; Peng, L. M. *Acta Crystallogr.* **2002**, *B58*, 587−593.
(27) Ma, R.; Bando, Y.; Sasaki, T. *Chem. Phys. Lett.* **2003**, *380*, 577−582.